

Adaptive Control Strategy for Low Voltage Ride Through Capability Enhancement of A Grid-Connected Switched Reluctance Wind Generator

*Hany M. Hasanien**, *S. M. Muyeen[†]*, and *Ahmed Al-Durra[†]*

**Electrical Power and Machines Department, Faculty of Engineering, Ain Shams University, Cairo 11517, Egypt (hanyhasanien@ieee.org),[†]Department of Electrical Engineering, The Petroleum Institute, Abu Dhabi 2533, UAE*

Keywords: Adaptive controller, low voltage ride through, switched reluctance generator, variable-speed wind turbine.

Abstract

This paper presents the application of an adaptive control strategy to enhance the low voltage ride through (LVRT) capability of a grid-connected switched reluctance wind generator. In this study, the switched reluctance generator (SRG) is driven by a variable-speed wind turbine and connected to the grid through an asymmetric half bridge inverter, DC-link, and DC-AC inverter system. The adaptive proportional-integral (PI) controllers are used to control the power electronic circuits. The Widrow-Hoff adaptation algorithm is used in this study. The Widrow-Hoff delta rule can be used to adapt the PI controllers' parameters. The detailed modelling and control strategies of the overall system are presented. The effectiveness of the proposed control scheme is verified under a severe symmetrical grid fault condition. The validity of the proposed system is verified by the simulation results, which are carried out using PSCAD/EMTDC.

1 Introduction

THE RENEWABLE energy systems have received a great attention worldwide as alternative energy sources due to the increase in fuel price, political issues, and environmental concerns. It is expected that the renewable energy will generate more than 25% of world's electricity by 2035 [1]. A quarter of this amount will be generated from the wind energy which is the second largest renewable energy source after hydro power. Based on the Global Wind Energy Council statistics, more than 35 GW of new wind power stations were installed in 2013. The global wind power installation capacity reach 318.105 GW at the end of 2013, representing a cumulative market growth of more than 12.5% [1]. As a result of the high level of penetration of the wind power into the electric grids, many problems including low voltage ride through arise in the electric power systems. These problems should be addressed, studied, and investigated adequately. Therefore, it is needed to enhance low voltage ride through (LVRT) capability of grid-connected wind generators.

The requirement of the LVRT applies to the wind power generators in order to remain stable and connected to the grid at grid fault conditions. Any disconnection of the wind power generators perhaps causes a critical grid situation and reduces the security standards especially when the wind penetration level is high. The recent wind farm grid codes insist on the LVRT characteristics of the wind power generators [2]. As a result of US recent wind farm grid codes, the wind farm terminal voltage must return to 90% of the rated voltage within 3 s after the start of the voltage drop, otherwise, the wind farm power station has to be shutdown.

The variable-speed wind turbine generator system (WTGS) has recently become more popular than that of fixed-speed. In 2004, the world-wide market share of the variable-speed WTGS was more than 60% [3]. The doubly fed induction generator (DFIG), wound field synchronous generator (WFSG), and permanent magnet synchronous generator (PMSG) are currently used as variable-speed wind generators. Besides the aforementioned classical machines used in variable-speed operation of WTGS, the switched reluctance generator (SRG) has some superior characteristics suitable for wind power applications. The SRG is a doubly salient, singly-excited generator. It has an unequal number of salient poles on both the rotor and the stator, but only one member (usually the stator) carries windings, and each two diametrically poles usually form one phase. The rotor has no winding, magnets, or cage winding and is built up from a stack of salient-pole laminations. The SRG possesses many inherent advantages such as simplicity, robustness, low manufacturing cost, high speed, and high efficiency [4]-[7]. It is also possible to operate the SRG in variable-speed mode. To date, these applications include sourcing aerospace power systems [8], automotive applications [9], [10], hybrid vehicles [11], and wind turbine applications [12]-[16]. The aerospace and automotive applications are generally characterized by high speed operation. The wind energy application is characterized by low speed, high torque operation. In [12], the advantage of the SRG for wind energy application was reported well, though the control strategy was unfocused. The one phase reluctance generator was proposed for wind energy conversion in [13]. In [14], the grid interfacing of wind energy conversion system was not considered. The authors reported the extension of [14] into [15] considering grid interfacing and buck converter based topologies for generator

side control of SRG. In [16], sensorless control of SRG has been focused though the overall control strategy of SRG-WTGS has not been presented.

In this paper, detailed modeling and an adaptive control strategy are developed to improve the LVRT of a grid-connected SRG, which is driven by a variable-speed wind turbine. For supplying power to the SRG, a voltage source topology is preferred and thus adopted in this study, which gives well defined voltages over semiconductors and SRG-phases. The premise of a voltage source topology implies a unipolar DC-link voltage with a relatively large DC-link capacitor as a temporary energy buffer. The asymmetric half bridge inverter based on hysteresis control is considered herein for the generator side control of the SRG. The Widrow-Hoff algorithm based adaptive PI controller is considered to control the switching on angle of the SRG to run the generator at the optimum speed of variable-speed wind turbine that ensures the maximum power extraction from the wind. The effectiveness of the proposed control scheme is verified under a severe symmetrical grid fault condition. The validity of the proposed system is verified by the simulation results, which are carried out using PSCAD/EMTDC.

2 Wind Turbine Modelling

The mathematical relation to the mechanical power extraction from the wind can be expressed as follows [17]-[26]:

$$P_M = 0.5\rho C_p(\lambda, \beta)\pi R^2 V_w^3 [W] \quad (1)$$

where P_M is the extracted power from the wind, ρ is the air density [kg/m^3], R is the blade radius [m], V_w is the wind speed [m/s], and C_p is the power coefficient which is a function of both tip speed ratio, λ , and blade pitch angle, β [deg]. C_p is expressed by the following equations:

$$C_p(\lambda, \beta) = 0.5(\Gamma - 0.02\beta^2 - 5.6)e^{-0.17\Gamma} \quad (2)$$

$$\lambda = \frac{\omega_m R}{V_w}, \quad \Gamma = \frac{R}{\lambda} \cdot \frac{3600}{1609} \quad (3)$$

where ω_m is the rotational speed [rad/s].

In variable-speed WTGS, the generated active power depends on the power coefficient, C_p , which is related to the proportion of power extracted from the wind. The optimum values of the tip speed ratio and power coefficient are chosen constant values based on the turbine characteristics. For each instantaneous wind speed of VSWT, there is a specific turbine rotational speed, ω_r , which corresponds to the maximum active power, P_{\max} , from the wind generator. In this study, power coefficient curve with maximum power point tracking (MPPT) line is shown in Fig. 1. Since the precise measurement of the wind speed is difficult, it is better to calculate the maximum power, P_{\max} , without the measurement of wind speed as shown below.

$$P_{\max} = 0.5\rho\pi R^2 \left(\frac{\omega_r R}{\lambda_{\text{opt}}} \right)^3 C_{p_{\text{opt}}} \quad (4)$$

From Eq. (4), it is clear that the maximum generated power is proportional to the cube of rotational speed. The pitch

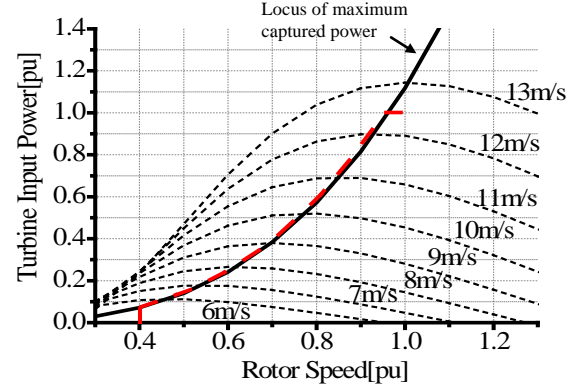


Fig. 1. Wind turbine characteristics for variable-speed operation

converter works when the rotor speed exceeds the rated speed to control the mechanical torque of wind turbine.

3 SRG Modelling Including Generator Side Converter

The switched reluctance machine is operated in the generating mode by positioning phase current pulses during periods where the rotor is positioned such that the phase inductance is decreasing. This occurs immediately after the rotor and stator poles have passed alignment. Normally, in this generator mode, the machine obtains its excitation from the same voltage bus that it generates power to. Typically, a phase is turned on before a rotor pole aligns with that phase, drawing energy from the dc bus to excite the phase. Once the rotor pole passes alignment with the phase's stator pole the winding is disconnected from the dc bus. It then generates into this same bus through suitably connected diodes. The work done by the mechanical system to pull the rotor poles away from the stator poles is returned to the dc bus. The excitation energy plus additional generated energy is returned to the dc bus. The control key is to position the phase current pulses precisely timed [27]. The precise rotor position is very useful in order to maximize the efficiency and to reduce power ripple. Fig. 2 illustrates a three phase SRG inverter system with two controllable power semiconductor switches and two diodes per phase, and this circuit is called an asymmetric half bridge inverter for a 3-ph SRG. Thus each phase has pulse nature parameters (current, flux-linkage, and torque). The torque is produced by the tendency of the rotor poles to align with the stator poles of the excited windings, and it is independent of the phase current direction.

The model of the SRG for dynamic analysis is composed of set of phase circuit and mechanical differential equations. In integrating these equations, the problem centers on handling the data (flux-linkage/angle/current) used to describe the magnetic nature of the SRG [28]. Different methods have been used for numerical integration of the nonlinear differential equations of the SRG with the magnetization data in the form of a look-up table. In this study, the magnetization curves of the SRG are derived from the measured data. The

cubic spline interpolation technique is used, which is, in general, more accurate than other standard techniques and gives more smoothed representation of the magnetization curves. The magnetization characteristics are extended using the cubic spline interpolation algorithm to cover the interval of rotor angles between the unaligned and the aligned positions as shown in Fig. 3. The co-energy curves are calculated from the following equation by applying the trapezoidal rule in numerical integration [28]:

$$\mathbf{W}'(\theta, \mathbf{i}) = \int_0^{\mathbf{i}} \Psi(\theta, \mathbf{i}) d\mathbf{i} \Big|_{\theta=\text{const}} \quad (5)$$

The static torque curves of the SRG are computed by numerical differentiation of the co-energy using the following equation:

$$\mathbf{T}(\theta, \mathbf{i}) = \frac{\partial \mathbf{W}'(\theta, \mathbf{i})}{\partial \theta} \Big|_{\mathbf{i}=\text{const}} \quad (6)$$

The previous characteristics data are carried out using MATLAB toolboxes [29]. These characteristics are stored in the form of look-up tables and used in the laboratory standard power system simulator PSCAD/EMTDC. Thus there are two look-up tables for the flux-linkage and for the static torque characteristics available to use during the computation of the generator differential equations. The generator under study is a three phase, 6/4 SRG, and the rated power is 48 kW at 3000 rpm. The parameters are illustrated in Appendix.

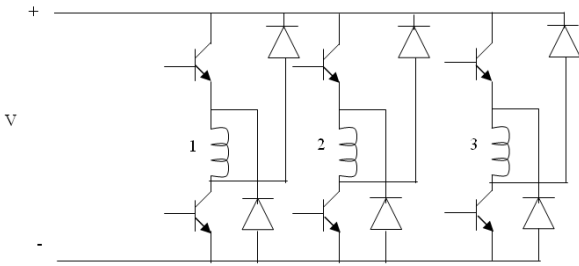


Fig. 2. Asymmetric half bridge inverter for a three-phase SRG.

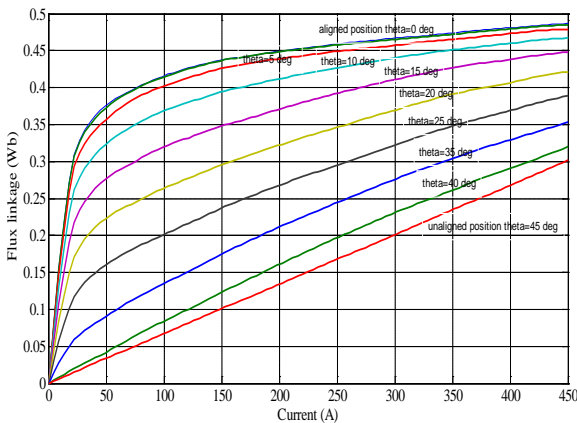


Fig. 3. Phase flux-linkage as a function of current and rotor position.

4 Control of The SRG Inverter

The control block diagram for the asymmetric half bridge inverter to generate gate pulse signals is shown in Fig. 4. The reference signal is determined from the maximum power

point tracking (MPPT) algorithm as explained in Sect. 2. The conduction signals are generated according to the logic explained as follows:

- The applied voltage (V) is positive during the conduction period, which is the difference between the switching off angle θ_{off} and the switching on angle θ_{on} .
- V is negative from θ_{off} until the extinction angle θ_{ext} which represents the angle corresponding to zero phase current.
- Otherwise, V equals zero.

The SRG rotor angular position, θ_r , is shifted by 30 degree in each phase for the 6/4 SRG. The hysteresis controller works well to generate the optimal firing angle for the inverter in order to maximize the output power of the generator according to the reference signal. In this study, the control technique is done using the adaptive PI controller.

a) PI Controller

The optimum speed is maintained by controlling the switching on angle, θ_{on} , as shown in Fig. 5, where ω_{r_opt} is the optimum rotational speed determined from MPPT. ω_{r_opt} is compared with the generator speed ω_r to yield the speed error $e(t)$. This error signal is the input of the PI controller. The output of the controller is a signal representing the incremental change in the switching on angle $\Delta\theta_{\text{on}}(t)$.

The equation of the PI controller can be written as follows:

$$\Delta\theta_{\text{on}}(t) = K_p \cdot e(t) + K_i \int e(t) \cdot dt \quad (7)$$

where K_p is the proportional gain, and K_i is the integral gain. The output signal of the PI controller $\Delta\theta_{\text{on}}(t)$ after being rescaled is used to modulate the generator phase switching on angle. The advanced switching-on angle $\theta_{\text{on_new}}$ can be written as follows:

$$\theta_{\text{on_new}}(t) = \theta_{\text{on_initial}} + k \cdot \Delta\theta_{\text{on}}(t) \quad (8)$$

where $\theta_{\text{on_initial}}$ is the initial switching on angle (5°), and k is a constant.

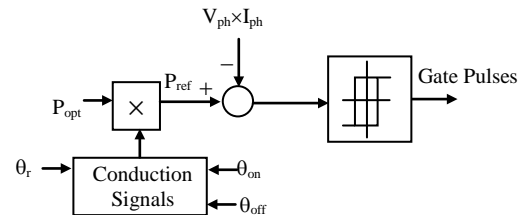


Fig. 4. Control block diagram for the SRG inverter

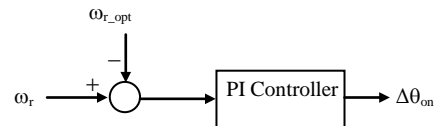


Fig. 5. Switching on angle control block diagram

b) Adaptation Algorithm

The adaptive PI controller is based on the Widrow-Hoff adaptation algorithm. The Widrow-Hoff delta rule, can be used to adapt the PI controllers' parameters. The delta rule,

which minimizes the mean square error of the generator speed can be written as [30]:

$$W(t+1) = \begin{cases} w(t) + \frac{\alpha \cdot e_w(t) \cdot x}{x^T \cdot x} & \text{if } x^T \cdot x \neq 0 \\ w(t) & \text{if } x^T \cdot x = 0 \end{cases} \quad (9)$$

Where $W(t+1)$ is the advanced gain at time $t+1$, $W(t)$ is the present gain at time t , x is the input vector, and α is the reduction factor. The speed error is converge if and only if $0 < \alpha < 2$ [31].

5 Control of The Grid Side Inverter

The control block diagram for the grid side inverter is shown in Fig. 6. It is based on the cascaded control scheme. The dq quantities and three-phase electrical quantities are related to each other by the reference frame transformation. The angle of the transformation is detected from the three phase voltages (v_a, v_b, v_c) at the high voltage side of the grid side transformer. The dc-link voltage can be controlled by the d-axis current. On the other hand, the reactive power of the grid side inverter can be controlled by the q-axis current. The reactive power reference is set in such a way that the terminal voltage at high voltage side of the transformer remains constant. The triangular signal is used as the carrier wave of the pulse width modulation (PWM) operation. The carrier frequency is chosen 1000 Hz.

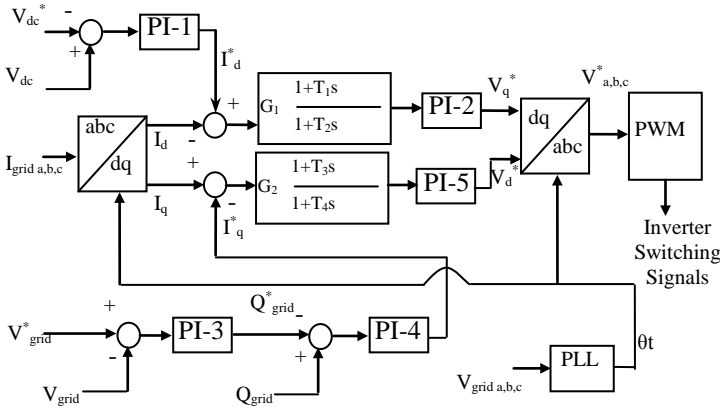


Fig. 6. Control block diagram for the grid side inverter

6 Model System

The model system used for the dynamic analysis of VSWT-SRG is shown in Fig. 7. Here one SRG is connected to an infinite bus through the asymmetric half bridge inverter, DC-link capacitor, grid side inverter, transformer, and double circuit transmission line. The system base is 48 kVA.

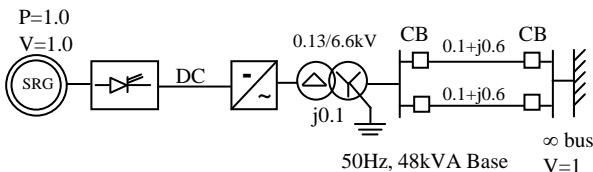
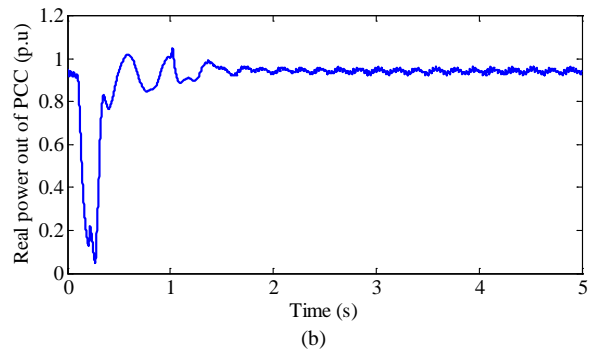
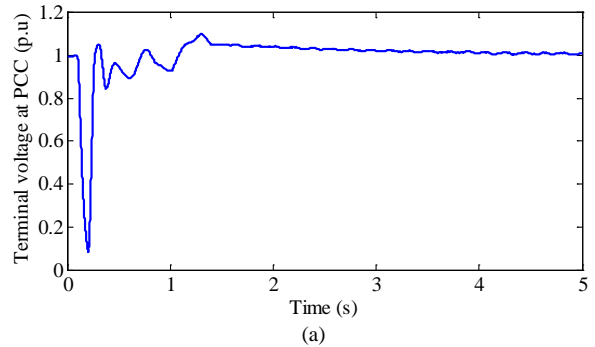


Fig. 7. Model System

7 Simulation Results

In this study, the detailed model of the system is considered. Time domain simulation has been carried out using PSCAD/EMTDC. The time step is chosen 10 μ s. It is assumed that wind speed is constant and equivalent to the rated speed. The wind farm grid code is fairly important to analyze the transient characteristics of WTGS. The wind farm grid codes are more or less similar in different countries with minor variations in voltage dip magnitude, fault time, voltage recovery time, etc., for the case of fault ride through standards. In this study, the simulation results are described in light of the grid code set by E. On Netz [2]. The FRT requirement is imposed on a wind power generator so that it remains stable and connected to the network during the network faults. The disconnection of the wind farm from the grid may worsen a critical grid situation and can threaten the security standards when the wind penetration is high.

In this study, the severe symmetrical three-line to ground fault (3LG) is considered as a network disturbance. The fault occurs at 0.1 s at the sending end of the transmission line, as shown in Fig. 7. The circuit breakers (CBs) on the faulted lines are opened at 0.2 s, and at 1 s the CBs are reclosed. The grid side inverter provides necessary reactive power during the network disturbance. Therefore, the terminal voltage at the point of common coupling (PCC) returns back to its pre-fault value, as shown in Fig. 8(a). From Fig. 8(a), it can be realized that the terminal voltage response is faster and better damped. The real and reactive power responses out of the PCC are shown in Figs. 8(b) and (c), respectively. The DC-link voltage response is shown in Fig. 8(d). Due to the DC-link over voltage protection circuit, the DC-link voltage can be maintained within an acceptable range. The response of current through braking chopper is shown in Fig. 8(e).



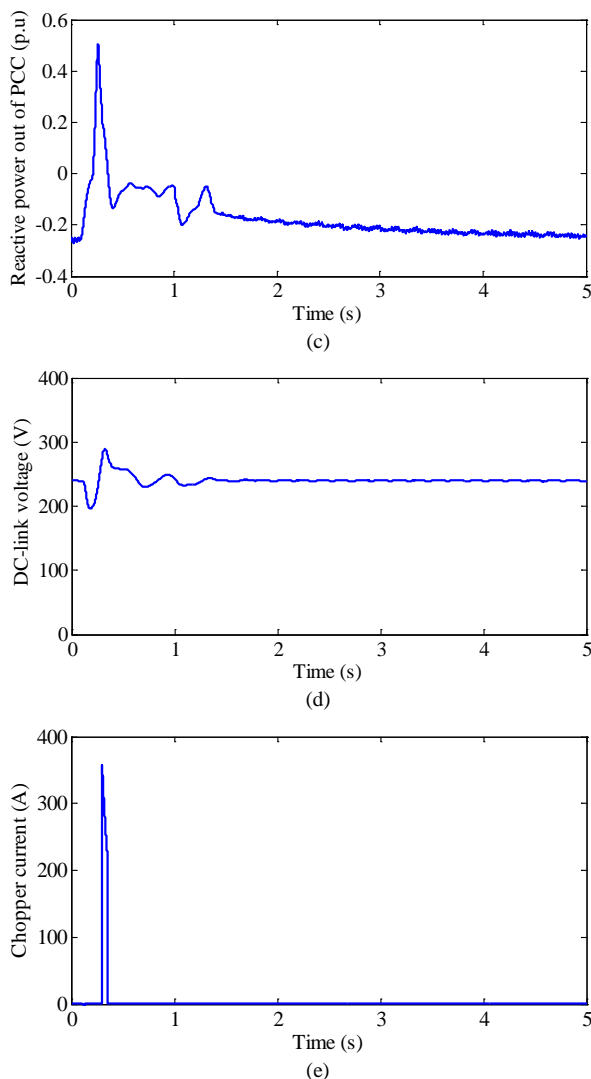


Fig. 8. Responses for 3LG fault (a) Terminal voltage at the PCC. (b) Real power out of the PCC. (c) Reactive power out of the PCC. (d) DC-link voltage. (e) The chopper current.

8 Conclusion

This paper has presented the application of an adaptive control strategy to enhance the LVRT capability of a grid-connected switched reluctance wind generator. The SRG is driven by a variable-speed wind turbine and connected to the grid through an asymmetric half bridge inverter, DC-link, and DC-AC inverter system. The adaptive PI controllers were successfully applied to control the power electronic circuits. The adaptation algorithm is based on the Widrow-Hoff delta rule. The simulation results have shown that the proposed adaptive PI controllers help improving the system responses without the need to fine tune the controllers' parameters. Therefore, the computational time and huge effort can be saved. It is found from the results that the terminal voltage at the PCC satisfies the LVRT requirements based on the recent wind farm grid codes. The proposed methodology is even suitable to other power system related applications such as FACTS devices, voltage source converter based HVDC system and so on, especially in the cases where it is difficult

to determine the suitable transfer function of a complex and larger system.

References

- [1] Global Wind Energy Council (GWEC), "Global Wind Report Annual Market Update 2013," online: <http://www.gwec.net>.
- [2] E. On Netz, Grid Code, High and Extra-High Voltage, April 2006, available at www.eon-netz.com/.
- [3] F. V. hulle, "Large scale integration of wind energy in the european power supply analysis, issue and recommendations," EWEA, Tech. Rep., December 2005.
- [4] T. J. E. Miller, "Switched reluctance motors and their control", Oxford University Press, 1993.
- [5] Hany M. Hasanien "Steady state performance of switched reluctance generator" *Journal of Electrical Engineering*, University Politehnica, Timisoara, Romania, vol. 8, no. 1, pp 53-60. April 2008.
- [6] Hany M. Hasanien, S. M. Muyeen, and Junji Tamura, "Torque ripple minimization of axial laminations switched reluctance motor provided with digital lead controller", *Energy Conversion and Management*, vol. 51, issue 12, pp. 2402-2406, Dec. 2010.
- [7] Eyhab El-Kharashi, and Hany M. Hasanien, "Reconstruction of the switched reluctance motor stator", *Journal of Electrical Engineering, Slovakia*, vol. 63. no. 1, pp. 1-10, January 2012.
- [8] D. E. Cameron and J. H. Lang, "The control of high-speed variable reluctance generators in electric power systems," *IEEE Transactions on Industry Applications*, vol. 29, no. 6, pp. 1106-1109, Nov./Dec. 1993.
- [9] M. Besbes, M. Gasbi, E. Hoang, M. Lecrivian, B. Grioni, and C. Plasse, "SRM design for starter-alternator system," in *Proc. Int. Conf. Electric Machines*, 2000, pp. 1931-1935.
- [10] C. Ferreira, S. R. Jones, W. Heglund, and W. D. Jones, "Detailed design of a 30-kw switched reluctance starter/generator system for a gas turbine engine applications," *IEEE Transactions on Industry Applications*, vol. 31, no. 3, pp. 553-561, May/June 1995.
- [11] J. M. Kokernak, D. A. Torrey and M. Kaplan, "A switched reluctance starter/ alternator for hybrid electric vehicles", *Power Electronics Proc. (PCIM) Conference*, pp. 74-80, 1999.
- [12] D. A. Torrey, "Variable reluctance generators in wind-energy systems," in *Proc. IEEE Power Electronics Specialists Conf.*, 1993, pp. 561-567.
- [13] L. Ribickis, E. Kamolins, N. Levin, and V. Pugachev, "One-Phase Reluctance Generators in Low-Power Wind Plants," *12th European Conference on Power Electronics and Applications (EPE2007)*, September 2007.
- [14] R. Cardenas, W. F. Ray, and G.M. Asher, "Switched reluctance generators for wind energy applications," in *Proc. IEEE Power Electronics Specialists Conf. (PESC95)*, 1995, pp. 559-564.
- [15] Roberto Cardenas, Ruben Pena, Marcelo Perez, Jon Clare, Greg Asher, and Patrick Wheeler, "Control of a switched reluctance generator for variable-speed wind energy applications," *IEEE Transactions on Energy Conversion*, vol. 20, no. 4, 2005.
- [16] E. Echenique, J. Dixon, R. Cárdenas, and R. Peña, "Sensorless control for a switched reluctance wind generator, based on current slopes and neural networks," *IEEE Transactions on Industrial Electronics*, vol. 56, no. 3, pp. 817-825, March 2009.
- [17] Hany M. Hasanien and S. M. Muyeen, "Design optimization of controller parameters used in variable-speed wind energy conversion system by genetic algorithms", *IEEE Transactions on Sustainable Energy*, vol. 3, no. 2, pp. 200-208, April 2012.
- [18] S.M. Muyeen, Hany M. Hasanien, and J. Tamura, "Reduction of frequency fluctuation for wind farm connected power systems by an adaptive artificial neural network controlled energy capacitor system", *IET Renewable Power Generation*, vol. 6, no. 4, pp. 226-235, July 2012.
- [19] Hany M. Hasanien, "A set-membership affine projection algorithm-based adaptive-controlled SMES units for wind farms output power smoothing", *IEEE Transactions on Sustainable Energy*, vol. 5, no. 4, pp. 1226-1233, October 2014.
- [20] Hany M. Hasanien, "Shuffled frog leaping algorithm-based static synchronous compensator for transient stability improvement of a grid-connected wind farm", *IET Renewable Power Generation*, vol. 8, no. 6, pp. 722-730, August 2014.
- [21] S. M. Muyeen, Hany M. Hasanien, and Ahmed Al-Durra, "Transient stability enhancement of wind farms connected to a multi-machine

power system by using an adaptive ANN-controlled SMES”, *Energy Conversion and Management*, vol. 78, no. 2, pp. 412-420, February 2014.

[22] Hany M. Hasanien, and S. M. Mueeen, “A Taguchi Approach for Optimum Design of Proportional-Integral Controllers in Cascaded Control Scheme”, *IEEE Transactions on Power Systems*, vol. 28, no. 2, pp. 1636-1644, May 2013.

[23] Hany M. Hasanien, and Essam. A. Al-Ammar, “Dynamic response improvement of doubly fed induction generator based wind farm using fuzzy logic controller”, *Journal of Electrical Engineering, Slovakia*, vol. 63, no. 5, pp. 281-288, September 2012.

[24] Hany M. Hasanien and S. M. Mueeen, “Affine projection algorithm based adaptive control scheme for operation of variable speed wind generator”, *IET Generation, Transmission and Distribution*, vol. 9, no. 16, pp. 2611-2616, 2015.

[25] Talha A. Taj, Hany M. Hasanien, A. I. Alolah, and S. M. Mueeen, “Transient stability enhancement of a grid-connected wind farm using an adaptive neuro-fuzzy controlled-flywheel energy storage system”, *IET Renewable Power Generation*, vol. 9, no. 7, pp. 792-800, 2015.

[26] M. N. Ambia, Hany M. Hasanien, A. Al-Durra, and S. M. Mueeen, “Harmony search algorithm-based controller parameters optimization for a distributed-generation system,” *IEEE Transactions on Power Delivery*, vol. 30, no. 1, pp. 246-255, February 2015.

[27] Iqbal Husain, Arthur Radun, and John Nairus, “Fault analysis and excitation requirements for switched reluctance generators,” *IEEE Transactions on Energy Conversion*, vol. 17, no. 1, pp. 67-72, March 2002.

[28] Hany M. Hasanien, and S. M. Mueeen, “Speed control of grid-connected switched reluctance generator driven by variable speed wind turbine using adaptive neural network controller”, *Electric Power Systems Research*, vol. 84, no. 1, pp. 206-213, March 2012.

[29] Release 2013 a, “MATLAB,” The Math Works press, February 2013.

[30] Hany M. Hasanien, S. M. Mueeen, and Junji Tamura, “Speed control of permanent magnet excitation transverse flux linear motor by using adaptive neuro-fuzzy controller”, *Energy Conversion and Management*, vol. 51, issue 12, pp. 2762-2768, Dec. 2010.

[31] Hany M. Hasanien, “FPGA implementation of adaptive ANN controller for speed regulation of permanent magnet stepper motor drives”, *Energy Conversion and Management*, vol. 52, issue 2, pp. 1252-1257, Feb. 2011.

APPENDIX

The SRG specifications are illustrated in Table I.

TABLE I
SRG SPECIFICATIONS

The phase winding resistance	0.05 Ω
The DC supply voltage	240 V
The maximum phase current	200 A
The rated torque	152.79 N.m
The rated speed	3000 rpm
The rated power	48 kW
No. of motor phases	3
The rotor moment of inertia	0.05 Kg.m ²
The friction coefficient	0.02 N.m.s